ACS APPLIED MATERIALS & INTERFACES

Research Article

www.acsami.org

Inorganic Nanoparticle Thin Film that Suppresses Flammability of Polyurethane with only a Single Electrostatically-Assembled Bilayer

Debabrata Patra, Prithvi Vangal, Amanda A. Cain, Chungyeon Cho, Oren Regev,[‡] and Jaime C. Grunlan*,[†]

[†]Department of Mechanical Engineering and Department of Material Science and Engineering, Texas A&M University, College Station, Texas 77843, United States

[‡]Department of Chemical Engineering, Ben-Gurion University of the Negev, Beer-Sheva, Israel, 8410501

Supporting Information

ABSTRACT: In an effort to reduce the flammability of polyurethane foam, a thin film of renewable inorganic nanoparticles (i.e., anionic vermiculite [VMT] and cationic boehmite [BMT]) was deposited on polyurethane foam via layer-by-layer (LbL) assembly. One, two, and three bilayers (BL) of BMT-VMT resulted in foam with retained shape after being exposed to a butane flame for 10 s, while uncoated foam was completely consumed. Cone calorimetry confirmed that the coated foam exhibited a 55% reduction in peak heat release rate with only a single bilayer deposited. Moreover, this protective nanocoating reduced total smoke release by 50% relative to untreated foam. This study revealed that 1 BL, adding just 4.5 wt % to PU foam, is an effective and conformal flame retardant coating. These results demonstrate one of the most efficient and renewable nanocoatings prepared using LbL assembly, taking this technology another step closer to commercial viability.

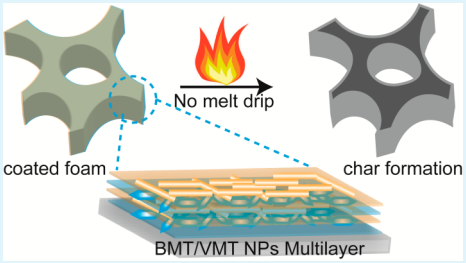

KEYWORDS: *layer-by-layer assembly, polyurethane foam, flame retardant, clay, boehmite, vermiculite, multilayer*

INTRODUCTION

The extensive use of flexible polyurethane (PU) foam in bedding, household furnishings, packaging, and automobiles has created an unintended fire hazard. Because of its chemical nature, air permeability and high burning velocity, PU foam is highly flammable.[1,2] In an effort to meet various fire regulation standards, PU foams are often filled with flame retardant materials to limit their flammability and to provide longer escape times in the event of fire.[3] Organohalogen compounds continue to be the most commonly used flame retardants for foam and they have played a critical role in reducing number of fire related fatalities and property damage.[4] Nevertheless, growing concerns about the potential negative environmental and health impacts of these flame retardants has prompted efforts to find safer replacements.[5−7]

Layer-by-layer (LbL) nanocoatings have proven to be an effective means to impart nonhalogenated flame retardant materials to highly flammable substrates like polyurethane,[8−10] cotton,[11−13] nylon,[14] polycarbonate,[15] and PET fabric.[16,17] LbL assembly is a versatile and inexpensive method to prepare nanocomposite thin films via alternate adsorption of positively and negatively charged polyelectrolytes from aqueous solutions through noncovalent interactions.[18−24] This assembly process can make use of polymers,[25,26] nanoparticles,[27,28] and biomolecules[29,30] to deposit multilayer thin films without altering the bulk substrate mechanical properties. These films have recently demonstrated sensing,[31,32] drug delivery,[33,34] antireflection,[35,36] charge storage,[37,38] oxygen barrier,[39−41] and antimicrobial properties.[42,43] Flame retardant nanocoatings prepared with this technique continue to attract immense interest due to easy fabrication, relatively safe chemistry and tremendous efficacy.[8−17,44−47] LbL deposition of polymer−clay or polymer−small molecule thin films (<100 nm) on foams or cotton, respectively, can completely extinguish flame and significantly reduces heat release rate (>50%) when exposed to flame. These nanocoatings form either a char-promoting thermal barrier, in the case of polymer−clay composites,[9,46] or extinguish fire by an intumescent mechanism in the case of polymer−polymer composites.[11,47] The only significantly drawback of the previously reported LbL coatings is the number of bilayers (each positive and negative pair deposited on the substrate is referred as a bilayer [BL]) necessary to impart a desired level of flame retardant performance, which increases processing cost.

In the present work, a highly efficient nanocoating comprised two naturally occurring inorganic nanoplatelets is studied. Cationic boehmite (BMT) and anionic vermiculite (VMT) were used to produce a thermally insulating barrier, as shown in Figure 1, which eliminates polyurethane foam melt-dripping and extinguishes fire. All three bilayers of these coatings (<20 nm thick) were effective enough to maintain the integrity of PU foam upon 10s exposure to the direct flame from butane torch

Received: July 9, 2014
Accepted: September 11, 2014
Published: September 11, 2014

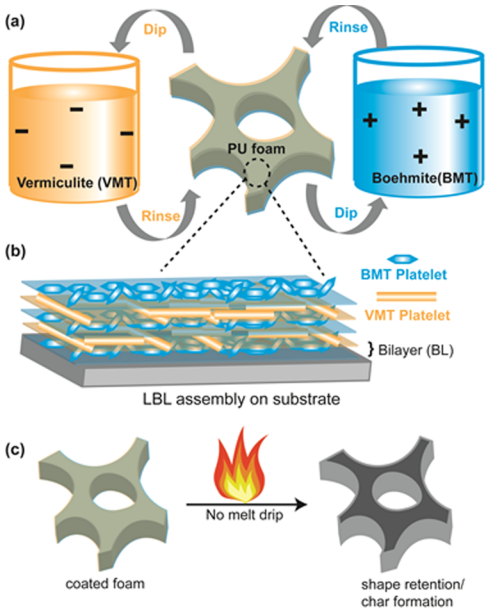

Figure 1. (a) Schematic of LbL assembly on PU foam using BMT and VMT. (b) A cross sectional schematic of the LbL assembled film on PU foam (particle size not to scale). (c) Flammability reduction of coated foam using butane torch test.

(Figure 1). A single BL nanocoating adds 4.5 wt % to the foam and reduces peak heat release rate (pkHHR) by 55% compared to an uncoated control in a cone calorimeter test. This unique "all inorganic" nanobrick wall provides an effective renewable flame retardant coating for complex substrates with very few layers, making it one of the most promising flame retardant recipes to-date.

EXPERIMENTAL SECTION

Materials. Natural vermiculite (trade name HTS-XE) clay, provided by Specialty Vermiculite Corp. (Cambridge, MA), was used as received. These nanoplatelets (~1 nm thick) have a negative surface charge in aqueous solution. An anionic solution was prepared by adding 1 wt % of vermiculite to deionized water and rolling. After 12 h, the solution was allowed to settle for 15 min in order to remove the insoluble aggregates. The unaltered supernatant was collected and measured to be pH ~7.5 with 1 wt % VMT. Light scattering suggests these platelets have an effective diameter of 1.1 μm. Boehmite nanoparticles ($AlOOH{\cdot}xH_2O$; B8013) were provided by Esprix Technologies (Sarasota, FL) and used as received. These cationic platelets have an average characteristic length of 180 nm in aqueous dispersion (crystallite size 30–60 nm; hexagonal schistose shape with a bulk density of 0.4–0.6 g/mL). The cationic solution was prepared by adding 0.5 wt % of boehmite to deionized water and rolling overnight. The pH of this solution was adjusted to 6 by adding 1 M NaOH prior to deposition. Branched polyethylenimine (PEI) (M_w = 25 000 g/mol, M_n = 10 000 g/mol) was purchased from Sigma–Aldrich (Milwaukee, WI). A 0.1 wt % PEI solution was prepared using 18.2 MΩ deionized water and rolling for 24 h. Poly(acrylic acid) (PAA), also purchased from Sigma-Aldrich (M_w = 100 000 g/mol, 35 wt % in water), was prepared as a 1 wt % solution using deionized water that was pH-adjusted to 2 using 2 M HNO_3.

Substrates. Ti–Au quartz crystals, with 5 MHz frequency (Maxtek, Inc., Cypress, CA), were used to monitor mass deposition per layer using a quartz crystal microbalance (QCM). QCM crystals were plasma cleaned in a PDC-32G plasma cleaner from Harrick Plasma (Ithaca, NY) for 5 min at 10.5 W, prior to use. P-doped, single side polished (1 0 0) silicon wafers (University Wafer, South Boston, MA), with a thickness of 500 μm, were used as substrates for ellipsometer thickness measurements. These wafers were cut to 4 × 1 in. and plasma cleaned under similar conditions. Melinex ST505 poly(ethylene terephthalate) (PET), with a thickness of 179 μm, was purchased from Tekra (New Berlin, WI) and used as the substrate for TEM imaging. The PET was rinsed with deionized water, methanol, and water again, then dried with filtered air and finally corona treated using a BD-20C Corona Treater (Electro-Technic Products, Inc., Chicago, IL). Polyether-based polyurethane foam (type 1850) with a density of 1.75 lbs/ft^3 was purchased from Future Foam (High Point, NC). This type of foam did not contain any flame retardant additives.

Layer-by-Layer Deposition. Treated substrates were dipped in the positively charged BMT solution for 5 min, rinsed in a stream of deionized water, and dried in a stream of filtered air. This procedure was followed by an identical dipping, rinsing and drying cycle in the VMT suspension. After this initial bilayer (BL) was deposited, the same procedure was followed with 1 min BMT and 1 min VMT dip times for each subsequent bilayer until the desired number of layers were deposited. Films measured with the ellipsometer, QCM, and TEM were placed in an oven for 1 h at 70 °C prior to characterization. To deposit BLs on polyurethane foam, a 4 × 4 × 1 in. piece was soaked in 1 wt % PAA for 30 s to induce a negative charge. The carboxylic acid groups on the PAA polymer chains remain largely protonated at pH 2 and hydrogen-bond to the polyurethane surface, depositing in a coiled, globular manner. After washing with DI water, the foam was soaked in 0.1 wt % PEI primer to impart a positive surface charge on the foam. Primer treated polyurethane foam was then soaked in oppositely charged VMT and BMT, respectively, for 1 min as described above (the initial bilayer was 5 min in each mixture). Each deposition was followed by the substrate being dip-rinsed in deionized water and wrung out to remove excess particles. All substrates were stored in a 0% RH box for a minimum of 18 h prior to testing.

Characterization. Film thickness was measured (on silicon wafers) using an alpha-SE Ellipsometer (J.A. Woollam Co., Inc., Lincoln, NE). Mass deposition was measured (on Ti/Au crystals) using a Research Quartz Crystal Microbalance (Maxtek, Inc., Cypress, CA). Control and coated foams were exposed to the direct flame of a butane micro hand torch (Model ST2200, Benzomatic, Huntersville, NC) for 10 s (the approximate blue flame temperature is 2400 °F) to provide a visual demonstration of coating effectiveness. Cone calorimetry was performed at the University of Dayton Research Institute, using a FTT Dual Cone Calorimeter, with a 35 kW/m^2 heat flux and an exhaust flow of 24 L/s, using a standardized procedure (ASTM E-1354-07). The samples were wrapped in aluminum foil on one side as required by ASTM E-1354-07.

Microscopic Imaging. Transmission electron microscope (TEM) samples were prepared by embedding the thin film (3 BL of nanocoating on 179 μm PET substrate) in Epofix resin (EMS, Hatfield, PA) overnight and cutting sections, using an Ultra 45° diamond knife (Diatome, Hatfield, PA), onto 300 mesh copper grids. TEM micrographs of the thin film cross sections (~50 nm thick) were imaged using a Tecnai G2 F20 (FEI, Hillsboro, OR) at an accelerating voltage of 200 kV. Coated thin films, deposited on PU substrates, were mounted on aluminum imaging stubs and thinly sputter coated with 5 nm of platinum/palladium (Pt/Pd) alloy in preparation for surface images that were acquired with a field-emission scanning electron microscope (FESEM) (Model JSM-7500F, JEOL; Tokyo, Japan). Surface topography was imaged with an atomic force microscope (AFM; Nanosurf Easy Scan 2 system, Nanoscience Instrument, Inc., Phoenix, AZ) in tapping mode.

RESULTS AND DISCUSSION

Nanocoating Growth and Microstructure. Thickness of BMT-VMT assemblies, as a function of bilayers deposited, was measured with ellipsometry, as shown in Figure 2a. The deposition is associated with electrostatic interaction between positively charged boehmite and negatively charged vermiculite platelets. This inorganic, nanoplatelet-based film exhibits linear growth with a thickness of ~150 nm for 30 BLs. The same trend was observed when growth was measured as a function of

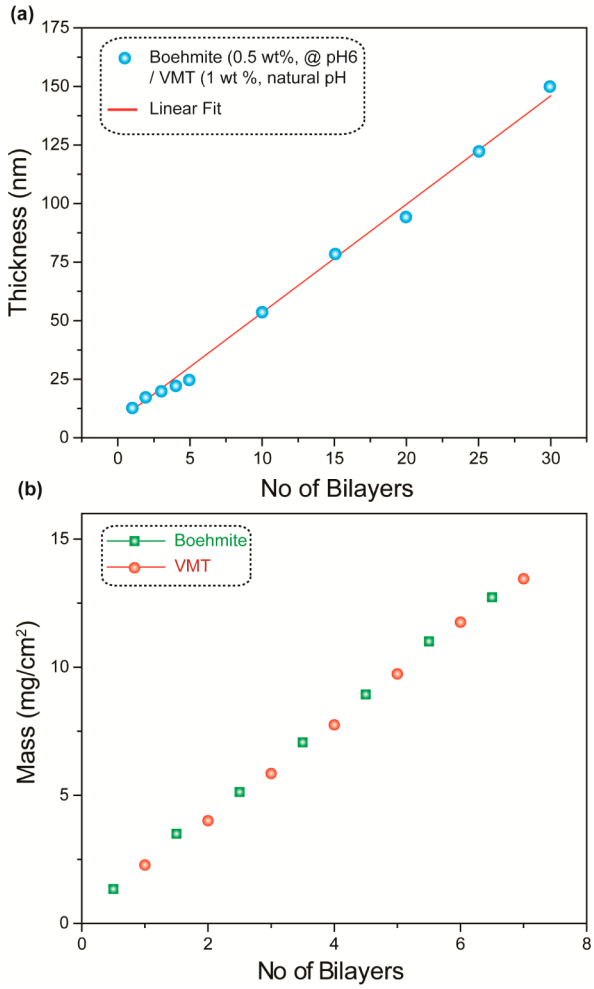

Figure 2. (a) Thickness and (b) mass of BMT-VMT assemblies as a function of bilayers deposited.

weight deposited (Figure 2b), using a quartz crystal microbalance. A semiquantitative assessment of thin film composition was obtained from QCM and it revealed the deposited film to be 38 wt % VMT and 62 wt % BMT. A high resolution TEM micrograph of a 3BL film, shown in Figure 3a, reveals the discrete multilayer nature of the VMT and BMT platelets (~300 and ~60 nm in length, respectively). The flexible VMT in the micrograph is shorter than its original length (~1000 nm), but sectioning is not necessarily performed along its longest length. Higher resolution micrographs of the VMT (Figure 3b) and BMT (Figure 3c) confirm characteristic *d*-spacings of 1.4 nm (001)[48] and 0.6 nm (111),[49] respectively, in agreement with the literature. There were fewer VMT layers observed than the number of deposition cycles (e.g., only two VMT layers are shown in Figure 3a, although 3 BLs were deposited). This seeming discrepancy could result from desorption of VMT platelets due to weak adhesion between the oppositely charged nanoparticles. The surface morphology of the thin film was imaged by AFM (Figure 3d), where phase contrast reveals partial coverage of VMT on top of the BMT layer, which supports the previous TEM analysis (Figure 3a). The RMS surface roughness was calculated (based on AFM images) to be 12 nm.

Flame Retardant Behavior on Polyurethane Foam. This BMT-VMT recipe was deposited onto flexible polyurethane foam with varying number of bilayers (1, 2, or 3). The weight added to the foam was determined by weighing before and after coating (reported as percentage of original mass). Figure 4 shows the SEM micrographs of uncoated and coated foam. The uncoated control is very smooth (Figure 4a), while coated foam has a rough nanotexture throughout the foam thickness that verifies the conformal nature of LbL deposition process. Figure 4c–h also shows the nanocoating texture getting thicker with increasing number of bilayers deposited. Foam flammability was initially tested by exposing samples to the direct flame from a hand-held butane torch for 10 s. The uncoated control foam ignited and started to melt drip immediately upon exposure to the flame, being completely consumed after removal of flame (see video in Supporting Information). No melt dripping was observed with any of the coated samples and the flame was extinguished after it traveled across the foam surface. A char was formed over the coated foam's surface with a complete retention of the original shape,

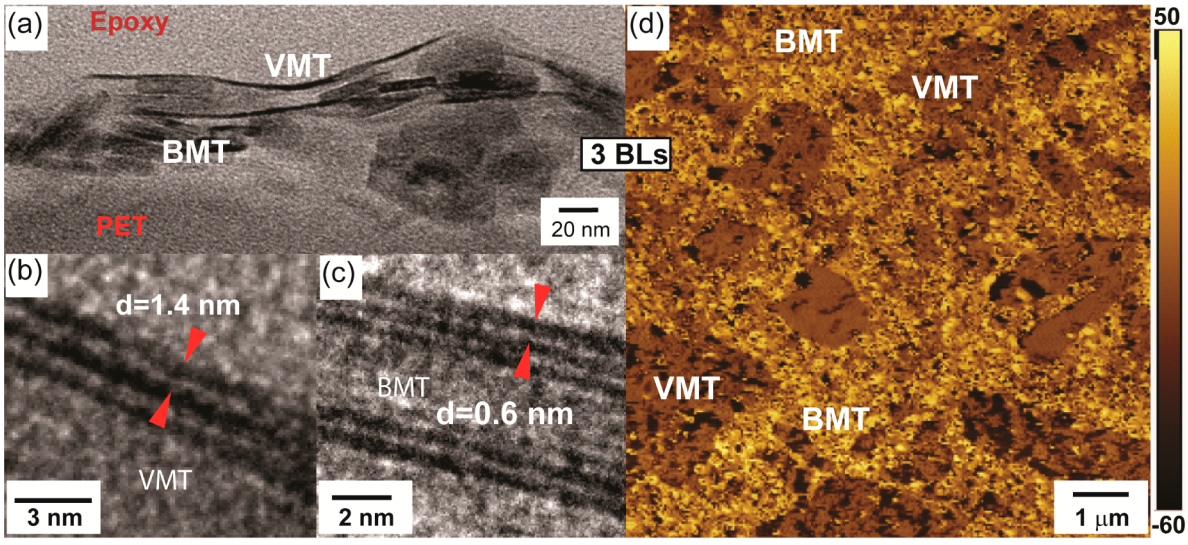

Figure 3. (a) TEM cross-sectional micograph of a 3BL assembly of boehmite and vermiculite. Characteristic *d*-spacing of (b) VMT and (c) BMT platelets. (d) AFM phase map of the film surface (RMS roughness ≈ 12 nm). The scale bar refers to phase (deg).

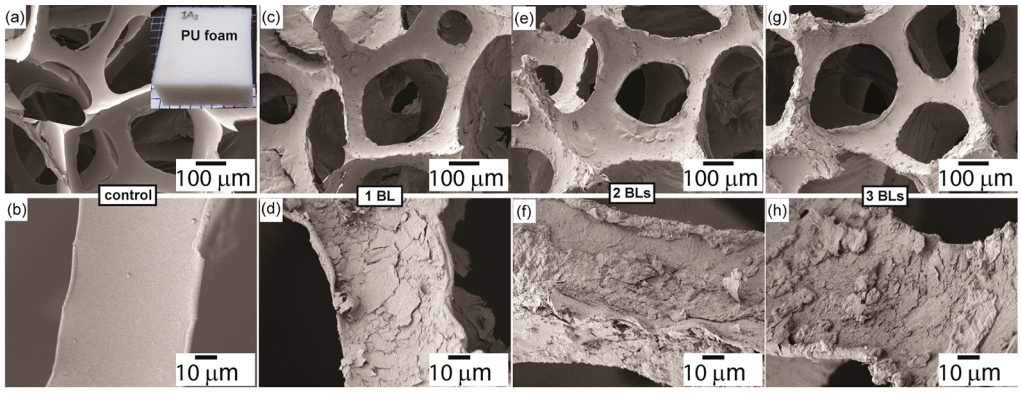

Figure 4. SEM images of control foam (a and b). Inset of panel a shows 2 × 2 in. PU foam used for coating. SEM images of coated foam: **1 BL** (c and d), **2 BL** (e and f), and **3 BL** (g and h).

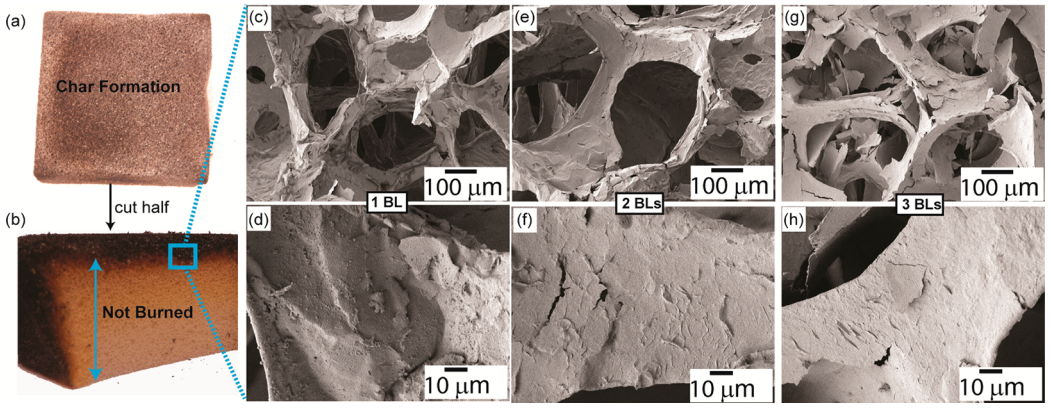

Figure 5. Digital micrographs of (a) charred foam and (b) vertically cut foam after butane torch exposure. SEM images of char residues: **1 BL** (c and d), **2 BL** (e and f), and **3 BL** (g and h).

as shown in Figure 5a. When cut through the middle, flexible, undamaged foam was observed underneath the char (Figure 5b). All the charred regions were analyzed by SEM, which revealed that the cells of the foam were distorted, but not completely damaged due to the presence of protective nanocoating (Figure 5c–h). All coated samples showed similar results, regardless the number of bilayers deposited (or weight gain). A single bilayer nanocoating added 4.5 wt % to the foam, while 3 bilayers added 8.8 wt %. Table 1 summarizes weight gain and char results from all samples tested. All three samples had similar char residue (~64 wt %) after the flame was extinguished.

In an effort to more quantitatively analyze the influence of BMT-VMT nanocoatings on polyurethane foam, cone calorimetry was performed on both coated and uncoated samples. Cone is a standard test to evaluate flammability under a constant external heat flux (35 kW/m^{-2}), which is meant to simulate a developing fire scenario. Figure 6 shows heat release rate (HRR) as a function of exposure time to this heat flux. The uncoated foam curve consists of two peaks associated with

Table 1. Butane Torch Test and Cone Calorimeter Results for Polyurethane Foam

sample	weight gain (%)	residue[a] (%)	pkHRR (kW/m^2)	total HR (MJ/m^2)	total smoke release (m^2/m^2)	MARHE (kW/m^2)
control			716	19.8	144	316
1 BL	4.5	63	340	18.5	77	190
2 BL	5.6	64	333	17.6	69	183
3 BL	8.8	66	342	18.3	69	191

[a]Char residue from butane torch test; pkHRR = peak heat release rate; release rate; total HR = total heat release; MARHE = maximum average rate of heat emission.

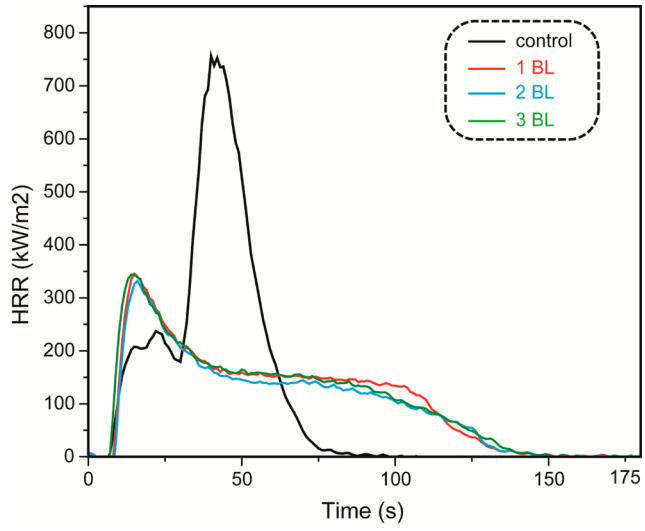

Figure 6. Heat release rate of BMT-VMT coated foam, and uncoated control, as a function of exposure time to 35 kW/m^2 heat flux in a cone calorimeter.

dx.doi.org/10.1021/am504455k | ACS Appl. Mater. Interfaces 2014, 6, 16903–16908

combustion of polyisocyanate (first peak at 20s) and polyol (second peak at 45s).[9] It should be noted that the coated foam samples had lower pkHRR (330−340 kW/m^2), but produced a higher first peak than the uncoated control. This larger first peak may be due to the presence the poly(acrylic acid) primer used to impart a negative surface charge to the foam and improve nanocoating adhesion. All coated samples were able to significantly diminish the second pkHRR, which indicates that a more durable residue was formed during combustion. More importantly, these nanocoatings were able to reduce peak heat release rate by 55% with a single bilayer (two bilayers was slightly better). Additionally, the hydrated nature of these nanomaterials (BMT and VMT) reduced total smoke release by 50% (see Table 1), which is just as important as heat release rate in many applications. It is well-known that the water present in these hydrated inorganics oxidizes carbon, thereby reducing the oxygen to fuel ratio and suppressing smoke formation during pyrolysis.[50]

Table 1 summarizes the important cone calorimeter parameters related to flammability of polyurethane foam that were greatly improved by these BMT-VMT nanocoatings. For example MARHE (maximum average rate of heat emission) is an ignition modified rate of heat emission, which can be used to rank material in terms of ability to support flame spread to other objects. There is no statistical significance in the decrease of total heat evolved (i.e., area under the HR curve) for both uncoated and coated samples. As noted above and supported by the data in Table 1, increasing the number of bilayers did not significantly improve the thermal stability of the open-celled foam. This was not surprising based on the patchy appearance of the 3 BL coating that has an uneven, cracked and flaking appearance (Figure 4). These LbL nanocoatings are believed to act as a condensed phase flame retardant that disrupts the pyrolysis process of the foam. Vermiculite and boehmite platelets create a "nanobrick wall" structure that effectively shields the foam from a heat source. Boehmite decomposes at 450 °C to release water vapor via an endothermic reaction that also serves as a heat sink to extinguish fire. During its degradation, boehmite transforms to aluminum trioxide (Al_2O_3) that can additionally act as an insulating barrier. Any open areas on the foam created by cracking and flaking would be expected to reduce the ability of the nanocoating to protect the foam. With no polymer between inorganic layers, this fully inorganic nanocoating is relatively weak from a mechanical standpoint. There is clearly room for improvement but the results shown here have demonstrated the ability of one or two bilayers, adding less than 6 wt % to the foam, to significantly reduce flammability.

CONCLUSIONS

LbL assembly of a fully inorganic nanoparticle coating was successfully applied to PU foam without altering open cell structure. The foam coated with a single BMT-VMT bilayer was able to self-extinguish the fire from a butane torch, with only the outermost surface being charred. Cone calorimetry revealed that this protective nanocoating reduced peak heat release rate, total smoke release and MARHE by a factor of 2, relative to uncoated foam. Foam coated with additional bilayers showed similar FR behavior, making it evident that 1 BL (4.5 wt % added to PU foam) is efficient enough to provide significant thermal protection. These results provide an opportunity for low cost, renewable, scalable, and efficient FR coatings on foam that could replace current halogenated FR additives.

ASSOCIATED CONTENT

Supporting Information

Torch test videos for coated and uncoated PU. This material is available free of charge via the Internet at http://pubs.acs.org/.

AUTHOR INFORMATION

Corresponding Author

*Tel: +1 979 845 3027; Fax: +1 979 862 3989; E-mail: jgrunlan@tamu.edu.

Notes

The authors declare no competing financial interest.

ACKNOWLEDGMENTS

The authors acknowledge the Fire Research Division (FRD) of the Engineering Laboratory (EL) at the National Institute of Standards and Technology (NIST) for financial support of this work, the Microscopy & Imaging Center (MIC) for TEM imaging assistance, and the Materials Characterization Facility (MCF) at Texas A&M for FESEM imaging assistance.

REFERENCES

(1) Lefebvre, J.; Bras, M.; Bastin, B.; Paleja, R.; Delobel, R. Flexible Polyurethane Foams: Flammability. *J. Fire Sci.* **2003**, *21*, 343−367.

(2) Hull, T. R.; Stec, A. A.; Polymers and Fire. In *Fire Retardancy of Polymers*, Hull, T. R., Kandola, B. K., Eds.; RSC Publishing: Cambridge, U. K., 2009; pp 1−14.

(3) Wang, J. Q.; Chow, W. K. A Brief Review on Fire Retardants for Polymeric Foams. *J. Appl. Polym. Sci.* **2005**, *97*, 366−376.

(4) de Wit, C. A. An Overview of Brominated Flame Retardants in the Environment. *Chemosphere* **2002**, *46*, 583−624.

(5) Watanabe, I.; Sakai, S. Environmental Release and Behavior of Brominated Flame Retardants. *Environ. Int.* **2003**, *29*, 665−682.

(6) Babrauskas, V.; Blum, A.; Daley, R.; Birnbaum, L. Flame Retardants in Furniture Foam: Benefits and Risks. *Fire Saf. Sci., Proc. Int. Symp.* **2011**, *10*, 265−278.

(7) Renner, R. Government Watch: EPA Won't Regulate Dioxin in Sewage Sludge. *Environ. Sci. Technol.* **2004**, *38*, 14A−15A.

(8) Laufer, G.; Kirkland, C.; Morgan, A. B.; Grunlan, J. C. Exceptionally Flame Retardant Sulfur-Based Multilayer Nanocoating for Polyurethane Prepared from Aqueous Polyelectrolyte Solutions. *ACS Macro Lett.* **2013**, *2*, 361−365.

(9) Cain, A. A.; Nolen, C. R.; Li, Y.; Davis, R.; Grunlan, J. C. Phosphorous-Filled Nanobrick Wall Multilayer Thin Film Eliminates Polyurethane Melt Dripping and Reduces Heat Release Associated with Fire. *Polym. Degrad. Stab.* **2013**, *98*, 2645−2652.

(10) Kim, Y. S.; Davis, R. Multi-walled Carbon Nanotube Layer-by-Layer Coatings with a Trilayer Structure to Reduce Foam Flammability. *Thin Solid Films* **2014**, *550*, 184−189.

(11) Li, Y.-C.; Mannen, S.; Morgan, A. B.; Chang, S.; Yang, Y.-H.; Condon, B.; Grunlan, J. C. Intumescent All-Polymer Multilayer Nanocoating Capable of Extinguishing Flame on Fabric. *Adv. Mater.* **2011**, *23*, 3926−3931.

(12) Huang, G.; Yang, J.; Gao, J.; Wang, X. Thin Films of Intumescent Flame Retardant-Polyacrylamide and Exfoliated Graphene Oxide Fabricated via Layer-by-Layer Assembly for Improving Flame Retardant Properties of Cotton Fabric. *Ind. Eng. Chem. Res.* **2012**, *51*, 12355−12366.

(13) Guin, T.; Krecker, M.; Milhorn, A.; Grunlan, J. C. Maintaining Hand and Improving Fire Resistance of Cotton Fabric through Ultrasonication Rinsing of Multilayer Nanocoating. *Cellulose* **2014**, *21*, 3023−3030.

(14) Apaydin, K.; Laachachi, A.; Ball, V.; Jimenez, M.; Bourbigot, S.; Toniazzo, V.; Ruch, D. Polyallylamine−Montmorillonite as Super

Flame Retardant Coating Assemblies by Layer-by Layer Deposition on Polyamide. *Polym. Degrad. Stab.* **2013**, *98*, 627−634.
(15) Carosio, F.; Blasio, A. D.; Alongi, J.; Malucelli, G. Layer by Layer Nanoarchitectures for the Surface Protection of Polycarbonate. *Eur. Polym. J.* **2013**, *49*, 397−404.
(16) Carosio, F.; Laufer, G.; Alongi, J.; Camino, G.; Grunlan, J. C. Layer-by-Layer Assembly of Silica-Based Flame Retardant Thin Film on PET Fabric. *Polym. Degrad. Stab.* **2011**, *96*, 745−750.
(17) Alongi, J.; Carosio, F.; Malucelli, G. Layer by Layer Complex Architectures Based on Ammonium Polyphosphate, Chitosan and Silica on Polyester−Cotton Blends: Flammability and Combustion Behaviour. *Cellulose* **2012**, *19*, 1041−1050.
(18) Decher, G. Polyelectrolyte Multilayers, An Overview. In *Multilayer Thin Films: Sequential Assembly of Nanocomposite Materials*, 2nd ed.; Decher, G., Schlenoff, J., Eds.; Wiley-VCH: Weinheim, Germany, 2012.
(19) Lvov, Y.; Decher, G.; Möhwald, H. Assembly, Structural Characterization, and Thermal Behavior of Layer-by-Layer Deposited Ultrathin Films of Poly(vinyl sulfate) and Poly(allylamine). *Langmuir* **1993**, *9*, 481−486.
(20) Costa, R. R.; Mano, J. F. Polyelectrolyte Multilayered Assemblies in Biomedical Technologies. *Chem. Soc. Rev.* **2014**, *43*, 3453−3479.
(21) Yang, M.; Hou, Y.; Kotov, N. A. Graphene-Based Multilayers: Critical Evaluation of Materials Assembly Techniques. *Nano Today* **2012**, *7*, 430−447.
(22) Ariga, K.; Yamauchi, Y.; Rydzek, G.; Ji, O.; Yonamine, Y.; Wu, C. W. K.; Hill, J. P. Layer-by-Layer Nanoarchitectonics: Invention Innovation and Evolution. *Chem. Lett.* **2014**, *43*, 36−68.
(23) Chapel, J. P.; Berret, J. F. Versatile Electrostatic Assembly of Nanoparticles and Polyelectrolytes: Coating, Clustering and Layer-by-Layer Processes. *Curr. Opin. Colloid Interface Sci.* **2012**, *17*, 97−105.
(24) Ariga, K.; Ji, Q.; Hill, J. P.; Bando, Y.; Aono, M. Forming Nanomaterials as Layered Functional Structures toward Materials Nanoarchitectonics. *NPG Asia Mater.* **2012**, *4*, e17.
(25) Bertrand, P.; Jonas, A.; Laschewsky, A.; Legras, R. Ultrathin Polymer Coatings by Complexation of Polyelectrolytes at Interfaces: Suitable Materials, Structure and Properties. *Macromol. Rapid Commun.* **2000**, *21*, 319−348.
(26) Kharlampieva, E.; Sukhishvili, S. A. Hydrogen-Bonded Layer-by-Layer Polymer Films. *J. Macromol. Sci., Polym. Rev.* **2006**, *46*, 377−395.
(27) Srivastava, S.; Kotov, N. Composite Layer-by-Layer (LBL) Assembly with Inorganic Nanoparticles and Nanowires. *Acc. Chem. Res.* **2008**, *41*, 1831−1841.
(28) Crespo-Biel, O.; Dordi, B.; Reinhoudt, D. N.; Huskens, J. Supramolecular Layer-by-Layer Assembly: Alternating Adsorptions of Guest- and Host-Functionalized Molecules and Particles Using Multivalent Supramolecular Interactions. *J. Am. Chem. Soc.* **2005**, *127*, 7594−7600.
(29) Hammond, P. T. Building Biomedical Materials Layer-by-Layer. *Mater. Today* **2012**, *15*, 196−206.
(30) Such, G. K.; Angus, P. R.; Johnston, A. P. R.; Caruso, F. Engineered Hydrogen-bonded Polymer Multilayers: From Assembly to Biomedical Applications. *Chem. Soc. Rev.* **2011**, *40*, 19−29.
(31) Lutkenhaus, J. L.; Hammond, P. T. Electrochemically Enabled Polyelectrolyte Multilayer Devices: From Fuel Cells to Sensors. *Soft Matter* **2007**, *3*, 804−816.
(32) Gao, Q.; Guo, Y.; Zhang, W.; Qi, H.; Zhang, C. An Amperometric Glucose Biosensor Based on Layer-by-Layer GOx-SWCNT Conjugate/Redox Polymer Multilayer on a Screen-Printed Carbon Electrode. *Sens. Actuators, B* **2011**, *153*, 219−225.
(33) Koker, S. D.; Hoogenboom, R.; De Geest, B. G. Polymeric Multilayer Capsules for Drug Delivery. *Chem. Soc. Rev.* **2012**, *41*, 2867−2884.
(34) Pavlukhina, S.; Sukhishvili, S. Polymer Assemblies for Controlled Delivery of Bioactive Molecules from Surfaces. *Adv. Drug Delivery Rev.* **2011**, *63*, 822−836.
(35) Zhang, L.; Li, Y.; Sun, J.; Shen, J. Layer-by-Layer Fabrication of Broad-band Superhydrophobic Antireflection Coatings in Near-infrared Region. *J. Colloid Interface Sci.* **2008**, *319*, 302−308.
(36) Hiller, J.; Mendelsohn, J. D.; Rubner, M. F. Reversibly Erasable Nanoporous Anti-reflection Coatings from Polyelectrolyte Multilayers. *Nat. Mater.* **2002**, *1*, 59−63.
(37) Jeon, J.; O'Neal, J.; Shao, L.; Lutkenhaus, J. L. Charge Storage in Polymer Acid-Doped Polyaniline-Based Layer-by-Layer Electrodes. *ACS Appl. Mater. Interfaces* **2013**, *5*, 10127−10136.
(38) Hyder, N.; Lee, S. W.; Cebeci, F. C.; Schmidt, D. J.; Shao-Horn, Y.; Hammond, P. T. Layer-by-Layer Assembled Polyaniline Nanofiber/Multiwall Carbon Nanotube Thin Film Electrodes for High-Power and High-Energy Storage Applications. *ACS Nano* **2011**, *5*, 8552−8561.
(39) Yang, Y.; Haile, M.; Park, Y. T.; Malek, F. A.; Grunlan, J. C. Super Gas Barrier of All-Polymer Multilayer Thin Films. *Macromolecules* **2011**, *44*, 1450−1459.
(40) Svagan, A. j.; Åkesson, A.; Cardenas, M.; Bulut, S.; Knudsen, J. C.; Risbo, J.; Plackett, D. Transparent Films Based on PLA and Montmorillonite with Tunable Oxygen Barrier Properties. *Biomacromolecules* **2012**, *13*, 397−405.
(41) Aulin, C.; Karabulut, E.; Tran, A.; Wagberg, L.; Lindström, T. Transparent Nanocellulosic Multilayer Thin Films on Polylactic Acid with Tunable Gas Barrier Properties. *ACS Appl. Mater. Interfaces* **2013**, *5*, 7352−7359.
(42) Dubas, S. T.; Kumlangdudsana, P.; Potiyaraj, P. Layer-by-Layer Deposition of Antimicrobial Silver Nanoparticles on Textile Fibers. *Colloids Surf., A* **2006**, *289*, 105−109.
(43) Lichter, J. A.; Van Vliet, K. J.; Rubner, M. F. Design of Antibacterial Surfaces and Interfaces: Polyelectrolyte Multilayers as a Multifunctional Platform. *Macromolecules* **2009**, *42*, 8573−8586.
(44) Carosio, F.; Blasio, A. D.; Cuttica, F.; Alongi, J.; Frache, A.; Malucelli, G. Flame Retardancy of Polyester Fabrics Treated by Spray-Assisted Layer-by-Layer Silica Architectures. *Ind. Eng. Chem. Res.* **2013**, *52*, 9544−9550.
(45) Kim, Y.; Li, Y.; Pitts, W. M.; Werrel, M.; Davis, R. D. Rapid Growing Clay Coatings to Reduce the Fire Threat of Furniture. *ACS Appl. Mater. Interfaces* **2014**, *6*, 2146−2152.
(46) Laufer, G.; Kirkland, C.; Cain, A. A.; Grunlan, J. C. Clay−Chitosan Nanobrick Walls: Completely Renewable Gas Barrier and Flame-Retardant Nanocoatings. *ACS Appl. Mater. Interfaces* **2012**, *4*, 1643−1649.
(47) Laufer, G.; Kirkland, C.; Morgan, A. B.; Grunlan, J. C. Intumescent Multilayer Nanocoating, Made with Renewable Polyelectrolytes, for Flame-Retardant Cotton. *Biomacromolecules* **2012**, *13*, 2843−2848.
(48) Righi, D.; Petit, S.; Bouchet, D. Characterization of Hydroxy-Interlayered Vermiculite and Illite/Smectite Interstratified Minerals from the Weathering of Chlorite in a Cryorthod. *Clays Clay Miner.* **1993**, *41*, 484−495.
(49) Liu, Y.; Han, X.; Bao, X.; Frandsen, W.; Wang, D.; Su, D. Hydrothermal Synthesis of Microscale Boehmite and Gamma Nanoleaves Alumina. *Mater. Lett.* **2008**, *62*, 1297−1301.
(50) Wilkie, C. A.; Morgan, A. B. *Fire Retardancy of Polymer Materials*; CRC Press: Boca Raton, FL, 2007; Chapter 7, pp 163−185.